Excellent near-UV emission and room-temperature ferromagnetism of square-like nano-CeO_2 mingled with $Ce(OH)_3$ synthesised by a hydrothermal method

Fanming Meng ✉, *Zhenghua Fan, Guodong Chen, Xin Yang*

Anhui Key Laboratory of Information Materials and Devices, Anhui University, Hefei 230601, People's Republic of China
✉ *E-mail: mrmeng@ahu.edu.cn*

Published in Micro & Nano Letters; Received on 3rd February 2016; Accepted on 23rd March 2016

Square-like nano-CeO_2 mingled with $Ce(OH)_3$ was successfully synthesised via a hydrothermal route using $CeCl_3{\cdot}7H_2O$ as cerium source, $N_2H_4{\cdot}H_2O$ as mineraliser, and ethylenediamine as complexant. The as-synthesised nanoparticles were characterised by X-ray diffraction, X-ray photoelectron spectroscopy, scanning electron microscope, high-resolution transmission electron microscopy, Raman scattering, photoluminescence spectra (PL), and magnetisation measurements. It was found that nano-CeO_2 has a fluorite cubic structure, and there are defects and vacancies in the sample. PL spectrum showed excellent near-UV emission. *M–H* curve exhibited excellent room-temperature ferromagnetism with saturation magnetisation of 0.0300 emu/g, coercivity of 73.706 Oe, and residual magnetisation of 2.37×10^{-3} emu/g, which can be mainly associated with the surface Ce^{4+}/Ce^{3+} pairs and oxygen vacancies in the nano-CeO_2.

1. Introduction: Ceria has drawn considerable attention because of their potential applications in spintronics, photocatalytic, gas sensors, energy and magnetic data storage and so on [1–4]. Ceria is a promising magnetic material due to its surface Ce^{4+}/Ce^{3+} pairs [5] and oxygen vacancies [6] favour the ferromagnetism (FM) order. It is well known that the control of morphology and size of nano-CeO_2 is of great interest due to the function of nanostructures mainly depends on their shape and dimension. Among numerous synthesis routes, a hydrothermal method is a facile and low-cost process for the synthesis of nano-CeO_2. In this Letter, we report on the room-temperature FM (RTFM) and near-UV emission of square-like nano-CeO_2 mingled with $Ce(OH)_3$ synthesised by a simple ethanol-assisted hydrothermal route.

2. Experimental

2.1. Material preparation: The growth of sample was performed dissolving 4 mmol $CeCl_3{\cdot}7H_2O$ in 20 ml ethanol and magnetic stirring, followed by dissolving 6 ml ethylenediamine with vigorous stirring for another 20 min. Then 4 ml $N_2H_4{\cdot}H_2O$ was dissolving to the solution and stirring for 15 min. Moreover, then obtained solution was put into a 50 ml Teflon-lined autoclave and heated for 8 h at 180°C. After being cooled to room temperature, the precipitate was collected by centrifugation, washed for three times using distilled water and ethanol, followed by drying in air for 10 h at 80°C.

2.2. Characterisation: The morphology was characterised with scanning electron microscope (SEM) (S-4800) and transmission electron microscopy (TEM) (JEM-2100). The selected area (electron) diffraction SAED and X-ray diffraction (XRD) (XD-3) were used to measure the crystalline phase of CeO_2 nanocolumns. The Raman spectrum was analysed using a Raman spectrometer system (inVia-Reflex) by an excitation laser of 532 nm at room temperature. The chemical states were studied using X-ray photoelectron spectroscopy (XPS) (ESCALAB 250 US Thermo Electron Co). The magnetic properties were measured at room temperature using a superconducting quantum interference device (MPMS XL-7). Photoluminescence (PL) spectra were examined with He–Cd laser of 325 nm as an excitation source. The radiation light was focused onto the entrance of a monochromator and the emission data were recorded by a charge coupled device detector.

3. Results and discussion: Fig. 1*a* presents the XRD pattern of the obtained nanoparticles. The peaks at 28.54°, 33.08°, 47.48°, 56.33°, 59.08°, 69.4°, 76.69°, 79.06°, and 88.41° are agreed with a fluorite cubic phase of CeO_2 (JCPDS Card No. 81-0792). The peaks at 15.54 and 39.54 can be agreed with $Ce(OH)_3$ (JCPDS Card No. 74-0665) with (1 0 0) and (2 0 1) planes, respectively. From the TEM image of Fig. 1*b*, it can be seen that the nanoparticles have a tendency of aggregate together due to big surface energy. So it is hard to say the size of nanoparticles because of agglomeration. The inset of Fig. 1*b* is the square-like nano-CeO_2 found in the TEM image. The HRTEM image in Fig. 1*c* shows that the CeO_2 nanostructures were mainly tiny nanoparticles with a diameter of 6–10 nm. Inset of Fig. 1*c* shows an SAED pattern measured from the agglomerated nanoparticles, presenting that the CeO_2 nanoparticles are polycrystalline. Moreover, the diffraction rings can be indexed to the CeO_2 of cubic phase. From the EDS spectrum of Fig. 1*d*, it can be seen that only singles of Ce and O elements were seen, which indicating no other element was introduced into the ceria during the synthesised process of the sample.

Fig. 2*a* shows the Ce3*d* XPS spectrum and its fitted deconvolutions of the as-synthesised nanoparticles. The peaks located at 881.85, 888.43, 897.58, 900.03, 907.53, and 916.99 eV are attributed to Ce^{4+} ions, while those at 883.99 and 903.10 eV are the characteristic peaks of Ce^{3+} [7]. This result implies that both Ce^{4+} and Ce^{3+} ions coexist, and there are surface Ce^{4+}/Ce^{3+} pairs in the CeO_2 nanocolumns. It was reported [8] that the Ce^{3+} ions distribute around oxygen vacancies in CeO_2. Fig. 2*b* shows Raman spectrum of the obtained nanoparticles measured at room temperature. The strong Raman peak centred at 461 cm^{-1} comes of Raman-active F_{2g} mode of CeO_2 cube phase [9], in other words, it originates from a stretching mode of the Ce-8O [10]. So, it is sensitive to disorder of oxygen sublattice resulted from doping, heat quantity, or grain-size effect [11]. The peak ranging from 560 to 600 cm^{-1} can be attributed to the presence of Ce^{3+} ions and oxygen vacancies [12]. This defect can induce magnetic moment in the nearby Ce^{3+} atoms. The Ce^{3+} has an electronic configuration belonging to partially filled 4f orbital with one unpaired electron contributing towards RTFM. The peak of 253 cm^{-1} can be attributed to the disorder in the system [13].

Fig. 3*a* shows *M–H* curve of the CeO_2, and the inset is the central part of Fig. 3. It can be seen that M_s (saturation magnetisation) is 0.03 emu/g, H_c (coercivity) is 73.706 Oe, and M_r (residual magnetisation) is 2.37×10^{-3} emu/g. The values of M_s are greater than the report of Li *et al.* [14], and the values of H_c and M_r are smaller than

doi: 10.1049/mnl.2015.0591

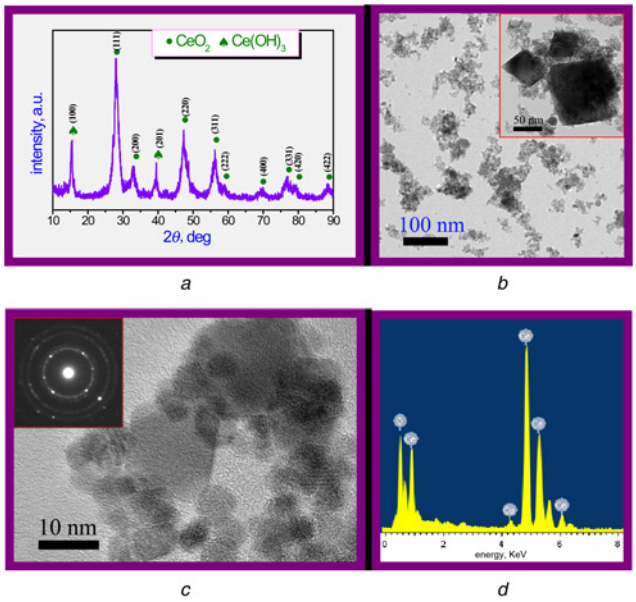

Fig. 1 *XRD pattern of the obtained nanoparticles*
a XRD
b TEM, inset is the square-like nano-CeO_2 found in the TEM
c HRTEM, inset is an SAED
d EDS of CeO_2 nanoparticles

the report of Liu *et al.* [2]. Obviously, the as-synthesised nanoparticles have excellent RTFM. From the analysis results of XPS and Raman, there are surface Ce^{4+}/Ce^{3+} pairs and oxygen vacancies in

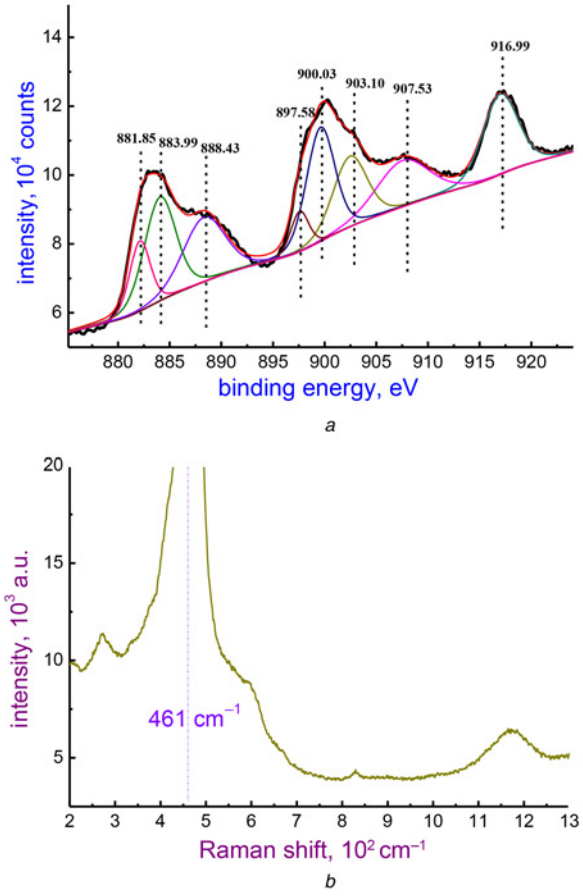

Fig. 2 *Ce3d XPS spectrum and its fitted deconvolutions*
a Ce3*d* XPS spectrum
b Room-temperature Raman spectrum of CeO_2 nanoparticles

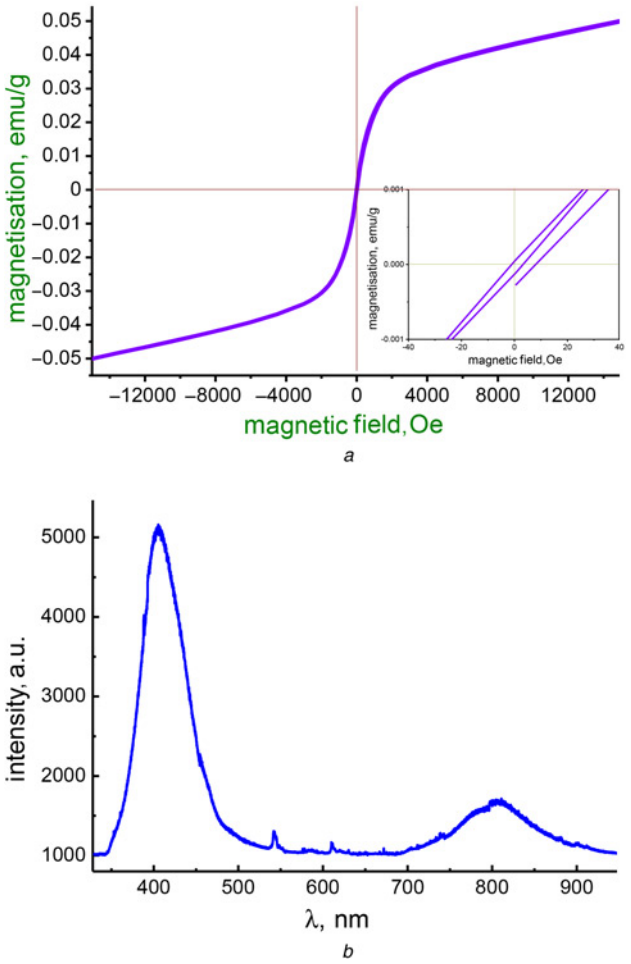

Fig. 3 *M–H curve of the CeO_2, and the inset is the central part*
a Room-temperature *M–H* curve
b Room-temperature PL spectrum of CeO_2 nanoparticles

the CeO_2 nanoparticles. As we know that, with the help of double-exchange mechanism, the surface Ce^{4+}/Ce^{3+} pairs could result in the charge transfer transition between Ce4*f* and O2*p* by enhance the hybridisation [15, 16], which favours FM order. In addition, as everyone knows that oxygen vacancy was assumed to cause RTFM [17]. So the RTFM of the obtained nanoparticles is likely associated with the effects of the oxygen vacancies and surface Ce^{4+}/Ce^{3+} pairs [18].

PL measurement was also performed using He–Cd laser of 325 nm as shown in Fig. 3*b*. A strong emission peak at around 405 nm dominates the spectra, which assigned to the UV excitonic emission. Aslam *et al.* reported [19] that the major peaks in the PL spectra of CeO_2 appeared at 470 nm. Wu *et al.* [20] reported that the major peaks in the PL spectra of CeO_2 appeared at 520 nm. The sample shows excellent UV emission compared to the above material. The other two emission peaks at 543 and 611 nm are weak, but still observable. It is not clear about the innate character of this appearance up to now. It is likely related to the oxygen vacancies provided with electronic energy levels under the Ce 4f or other localised defect states within the bandgap. Further investigations are needed to expound the beginning of these novel peaks.

4. Conclusion: In a word, square-like nano-CeO_2 mingled with $Ce(OH)_3$ has been prepared using a simple ethanol-assisted hydrothermal route. The obtained nanoparticles show good near-UV emission and RTFM with M_s of 0.0300 emu/g, H_c of 73.706 Oe, and M_r of 2.37×10^{-3} emu/g. The controllable morphologies, excellent near-UV emission and RTFM should

make the square-like nano-CeO_2 excellent roles in relevant fields. Meanwhile the ethanol-assisted hydrothermal route might provide a good method to synthesise other correlative materials and have latent industrial applications.

5. Acknowledgments: This work was supported by the Anhui Provincial Natural Science Foundation (grant no. 1508085SME219) and the College Students Research Training Program of Anhui University (grant no. J18520209) of China.

6 References

[1] Qian J.C., Chen Z.G., Liu C.B., *ET AL.*: 'Improved visible-light-driven photocatalytic activity of CeO_2 microspheres obtained by using lotus flower pollen as biotemplate', *Mater. Sci. Semicond. Process.*, 2014, **25**, pp. 27–33

[2] Liu Y.L., Lockman Z., Aziz A., *ET AL.*: 'Size dependent ferromagnetism in cerium oxide (CeO_2) nanostructures independent of oxygen vacancies', *J. Phys., Condens. Matter*, 2008, **20**, article id 165201

[3] Hardev S.S., Mukhtiyar S., Ali H.R., *ET AL.*: 'Accounting oxygen vacancy for half-metallicity and magnetism in Fe-doped CeO_2 dilute magnetic oxide', *Comput. Mater. Sci.*, 2013, **74**, pp. 114–118

[4] Carlos R.M., Alma H.M.: 'CO sensor based on thick films of 3D hierarchical CeO_2 architectures', *Sens. Actuators B*, 2014, **197**, article id 177

[5] Li M., Ge S.H., Qiao W., *ET AL.*: 'Relationship between the surface chemical states and magnetic properties of CeO_2 nanoparticles', *Appl. Phys. Lett.*, 2009, **94**, article id 152511

[6] Peng H.W., Xiang H.J., Wei S.H., *ET AL.*: 'Origin and enhancement of hole-induced ferromagnetism in first-row d0 semiconductors', *Phys. Rev. Lett.*, 2009, **102**, article id 017201

[7] Xu B., Zhang Q.T., Yuan S.S., *ET AL.*: 'Synthesis and photocatalytic performance of yttrium-doped CeO_2 with a porous broom-like hierarchical structure', *Appl. Catal. B, Environ.*, 2016, **183**, article id 361

[8] Marabelli F., Wachter P.: 'Covalent insulator CeO_2: optical reflectivity measurements', *Phys. Rev. B, Condens. Matter*, 1987, **36**, pp. 1238–1243

[9] Lu X.H., Huang X., Xie S.L., *ET AL.*: 'Facile electrochemical synthesis of single crystalline CeO_2 octahedrons and their optical properties', *Langmuir*, 2010, **26**, pp. 7569–7573

[10] Maensiri S., Masingboon C., Laokul P., *ET AL.*: 'Egg white synthesis and photoluminescence of plate like clusters of CeO_2 nanoparticles', *Cryst. Growth Des.*, 2007, **7**, pp. 950–955

[11] Kosacki I., Suzuki T., Anderson H.U., *ET AL.*: 'Raman scattering and lattice defects in nanocrystalline CeO_2 thin films', *Solid State Ion.*, 2002, **149**, pp. 99–105

[12] Mabride J.R., Hass K.C., Poindexter B.D., *ET AL.*: 'Raman and X-ray studies of $Ce_{1-x}RE_xO_{2-y}$, where RE=La, Pr, Nd. Eu, Gd and Tb', *J. Appl. Phys.*, 1994, **76**, pp. 2435–2441

[13] Kosacki I., Petrovsky V., Anderson H.U., *ET AL.*: 'Raman spectroscopy of nanocrystalline ceria and zirconia thin films', *Am. Ceram. Soc.*, 2002, **85**, pp. 2646–2650

[14] Li M., Zhang R., Zhang H., *ET AL.*: 'Synthesis, structural and magnetic properties of CeO_2 nanoparticles', *Micro Nano Lett.*, 2010, **5**, pp. 95–99

[15] Jiang Y., Adams J.B., Schilfgaarde M. van: 'Density-functional calculation of CeO_2 surfaces and prediction of effects of oxygen partial pressure and temperature on stabilities', *J. Chem. Phys.*, 2005, **123**, article id 064701

[16] Bensalem A., Muller J.C., Bozon-Verduraz F.: 'In-situ diffuse reflectance spectroscopy of supported cerium oxide', *J. Chem. Soc. Faraday Trans.*, 1992, **88**, pp. 153–159

[17] Venkatesan M., Fitzgerald C.B., Coey J.M.D.: 'Unexpected magnetism in a dielectric oxide', *Nature*, 2004, **430**, p. 630

[18] Meng F., Wang L.: 'Hydrothermal synthesis of monocrystalline CeO_2 nanopoles and their room temperature ferromagnetism', *Mater. Lett.*, 2013, **100**, pp. 86–88

[19] Aslam M., Qamar M.T., Salah N., *ET AL.*: 'The effect of sunlight induced surface defects on the photocatalytic activity of nanosized CeO_2 for the degradation of phenol and its derivatives', *Appl. Catal. B, Environ.*, 2016, **180**, pp. 391–402

[20] Wu L.N., Fang S.M., Ge L., *ET AL.*: 'Facile synthesis of Ag@CeO_2 core-shell plasmonic photocatalysts with enhanced visible-light photocatalytic performance T', *J. Hazards Mater.*, 2015, **300**, pp. 93–103

doi: 10.1049/mnl.2015.0591